PHYSICAL REVIEW A **78**, 011804(R) (2008)

Discrete cavity solitons due to saturable nonlinearity

A. V. Yulin,[1] A. R. Champneys,[1] and D. V. Skryabin[2]
[1]*Department of Engineering Mathematics, University of Bristol, Bristol, BS8 1TR, United Kingdom*
[2]*Center for Photonics and Photonic Materials, Department of Physics, University of Bath, Bath BA2 7AY, United Kingdom*
(Received 18 December 2007; published 15 July 2008)

Discrete localized structures are found in optical cavities with focusing saturable nonlinearity. Families of both bright and gray solitons exhibit multistability as they develop internal shelves in the pinning region around a Maxwell point. Both saturability and discreteness are required for these solitons to be observable, but they can occur for either zero or finite losses.

DOI: 10.1103/PhysRevA.78.011804 PACS number(s): 42.65.Tg, 05.45.Yv

Stationary localized structures in optical cavities containing a nonlinear material have received much attention due to their potential applications in optical information processing and intriguing physical properties [1]. These structures are commonly referred to as cavity solitons [1]. A rich plethora of stable cavity solitons have been shown to coexist due to the formation of *snaking* bifurcation diagrams in a proximity of the so-called Maxwell point (*pinning region*) where counterpropagating fronts connecting bistable homogeneous states lock one to another and form spatially localized bound states [2–6]. Recently, opportunities offered by nonlinear spatially periodic and discrete systems for manipulation by localized states of light have attracted significant attention. Models such as discrete nonlinear Schrödinger equations and various nonlinear equations with periodic potentials have been shown to support a range of stationary and moving localized structures, see, e.g., Refs. [7–11]. These studies have been extended to the models with loss and external driving or gain, such as occur in optical cavities with embedded photonic crystals and periodic arrays of optical cavities [12–15], where stable cavity solitons were found for the cases of cubic (Kerr) and quadratic nonlinearities.

The purpose of this Rapid Communication is to study effects of nonlinearity saturation on existence and stability of discrete cavity solitons. Unlike in the previously studied case of Kerr nonlinearity some of the solitons exist in the regime where the linear cavity detuning is not compensated by the nonlinearity detuning. Surprisingly enough these solutions even persist into the conservative (zero-dissipation) limit. We demonstrate that discreteness opens up certain intervals of parameters around Maxwell points in which stable versions of these solitons are born in snaking bifurcations. We also present a coherent explanation of why these families of discrete solitons are expected to exist in a wide class of discrete systems.

We consider an infinite array of coupled optical cavities governed by the dimensionless equations

$$i\partial_t A_n + \delta A_n - \frac{\alpha}{1+|A_n|^2}A_n + c(A_{n+1} + A_{n-1} - 2A_n) = P,$$

$$-\infty < n < \infty. \tag{1}$$

Here A_n is the complex amplitude of the field in the nth cavity, $c \geq 0$ is the coefficient of coupling between the neighboring oscillators, and P is the amplitude of the pump field. Independence of the pump parameter P from n corresponds to normal incidence of the spatially homogeneous pump wave. In general, both δ and α can be complex. Nonlinearity form is typical for a medium of the off-resonant two-level atoms. The real parts of δ and α represent frequency detuning and their imaginary parts account for the linear and nonlinear losses, respectively. We assume that α is real and positive, which corresponds to a focusing nonlinearity. We allow either Im $\delta=0$ (conservative case) or Im $\delta>0$ (lossy case).

Homogeneous solution $A_n(t)=A$ satisfies

$$\left(\delta - \frac{\alpha}{1+|A|^2}\right)A = P. \tag{2}$$

The equation above can have either one or three solutions, with the latter implying bistability between the low-intensity and high-intensity states. If $\mathrm{Im}(\delta)=0$ and $\alpha > \delta > 0$ then it is easy to show that bistability of the homogeneous solutions occurs for an interval of P values including $P=0$. If we add linear losses, then the bistability region starts at a nonzero pump value. All this is similar to the case of pure cubic nonlinearity. However, for $-\alpha/8 < \delta < 0$ bistability occurs as a direct consequence of the saturation effects, and starts at a pump value $P_{\min}$ different from zero, even in the conservative case: $P_{\min}=[\delta-\alpha/(1+|B|^2)]B$, where $B=\sqrt{[\alpha+2\delta+\sqrt{\alpha^2+8\delta\alpha}]/(-2\delta)}$. We focus below on the $\delta<0$ case, which is strikingly different from the previously studied focusing Kerr nonlinearity [12,13] exhibiting neither bistability nor localized structures for $\delta<0$.

In order for solitons to form on a given homogeneous background, the background state must be temporally stable. To find stable homogeneous states we look for the solution of Eq. (1) in the form $A_n=A+a_n(t)$, where a_n is small, and seek solutions in the form $a_n=\psi_+ e^{\lambda t+iqn}+\psi_-^* e^{\lambda^* t-iqn}$, with stability being implied by $\mathrm{Re}(\lambda)<0$. After some algebra we find

$$\lambda(q) = -\mathrm{Im}(\delta) \pm \sqrt{r^2|A|^4 - (\mathrm{Re}\{\delta + r + 2c[\cos(q)-1]\})^2}, \tag{3}$$

where $r=-\alpha/(1+|A|^2)^2$. This equation predicts stability of the lower and upper states of the bistability loop in the range $-\frac{\alpha}{8} < \delta < 0$ [see Fig. 1(c)].

We start our analysis of the localized structures from the simplest, but instructive, conservative case $\mathrm{Im}(\delta)=0$. We

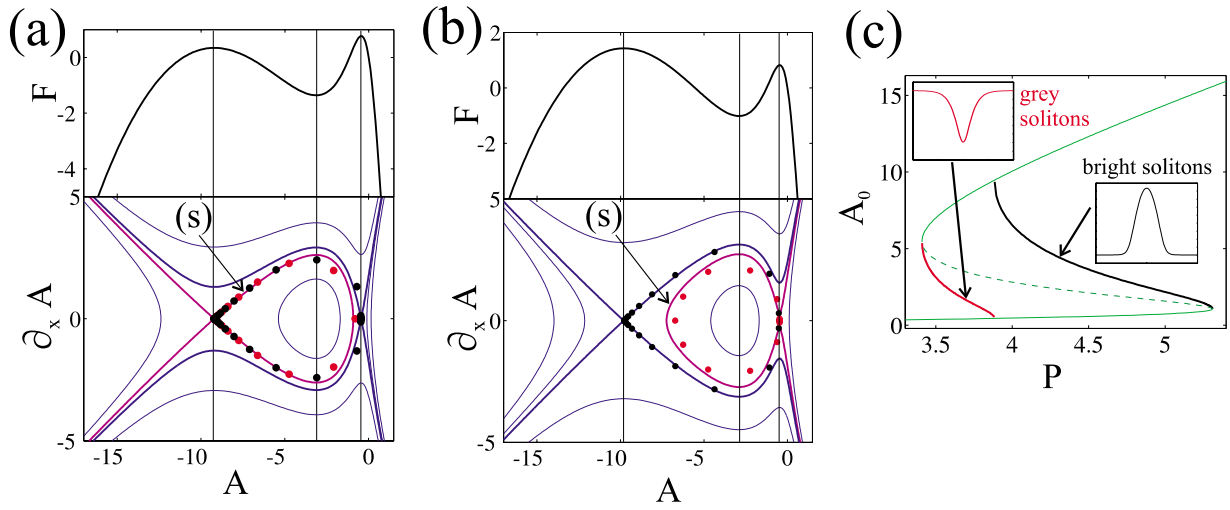

FIG. 1. (Color online) (a),(b) The potential and the corresponding phase plane for Eq. (4). The parameters are $\delta=-0.3$, $\alpha=10$, and $P=3.835$ (a), $P=3.95$ (b). The magenta lines [marked by (s)] in the phase planes show the separatrices of (a) the low-intensity and (b) the high-intensity soliton which indicate where the homoclinic orbits exist. The red and black circles show the numerically found fields of the discrete on-site solitons for the same parameters but for $c=0.5$; in that case the vertical axis is $(A_{n+1}-A_{n-1})/2$ and the horizontal axis is A_n. Note that there are infinitely many distinct discrete solitons for these fixed pumps. (c) The corresponding bifurcation diagram of homogeneous states (green line; with dashes representing instablility, solid stability) together with curves of the bright (black line) and gray (red line) solitons in the continuum limit $c\to\infty$.

consider the continuum limit $c\to\infty$, where $A_{n+1}+A_{n-1}-2A_n \to \partial_x^2 A$ and, without loss of generality, assume A to be real and satisfying

$$c\partial_x^2 A = -\frac{\partial F}{\partial A}, \quad F = \frac{\delta}{2}A^2 - \frac{\alpha}{2}\ln(1+A^2) - PA. \tag{4}$$

This equation describes the motion of a particle with mass c in the potential F. Figures 1(a) and 1(b) show the potential for two different values of P and the corresponding phase portraits of Eq. (4). The minimum of the potential corresponds to the intermediate state of the bistability curve, located between the two maxima, corresponding to the upper and lower bistable states. There is a critical value of $P=P_M$ (Maxwell point), such that the heights of the two maxima of F are the same. At this point a resting front connecting the bistable states exists in the system. At pump values close to the Maxwell point, the fronts still exist but they move. For $P<P_M$, the peak of F corresponding to the upper bistable state is the lower one. This implies existence of the homoclinic connection to this state, see Fig. 1(a), corresponding to the gray localized structure. The entire branch of these structures is shown in Fig. 1(c). For $P>P_M$, the peak corresponding to the lower bistable state is the lower one, meaning existence of the homoclinic connection to this state, corresponding to the bright localized structures, see Figs. 1(b) and 1(c). The bright solitons exist between the Maxwell point, where they can be considered as a superposition of the two infinitely separated fronts and the right-hand fold point of the bistability curve, where their profile tends uniformly to the lower homogeneous state. The situation for the gray soliton is symmetric, but with the left-hand fold point being involved, see Fig. 1(c).

Considering a discrete situation we take Eq. (1) with large, but finite, coupling c. Then we can consider Eq. (1) as a two-dimensional map with coordinates A_n and $(A_{n+1}-A_{n-1})/2$. Upper and lower bistable states correspond to *hyperbolic* (saddle) fixed points of such a map, whereas the intermediate state is an elliptic fixed point. Now, owing to the general theory of homoclinic connections to saddle points in the continuum limit [16], two fundamental homoclinic trajectories of the map will occur that are exponentially close (as a function of $1/c$) to the solitons found in the continuum limit. These we identify as being on-site centered and off-site centered. The on-site solitons have the symmetry $A_n=A_{-n}$ where, without loss of generality, we have placed the maximum intensity at $n=0$, and the off-site solitons have the symmetry $A_{-n}=A_{n+1}$. In Fig. 1 gray (red) and black circles represent the on-site soliton; the off-site ones look similar. As the coupling is strong, the discrete homoclinic points follow the separatrix trajectory closely. For weaker coupling, the divergence of the circles from the continuous homoclinic orbit becomes bigger. Note in addition that the Smale-Birkhoff homoclinic theorem (e.g., Ref. [17]) gives the existence of a *homoclinic tangle*. This in turn implies existence of infinitely many bound states of these discrete solitons. Henceforth we are not considering these bound states, but rather study bifurcations of initially single-peak fundamental cavity solitons.

Let us now take an example of bright solitons and deal with the moderate coupling $[c\sim O(1)]$ in the case $\delta<0$. Since the discrete homoclinic orbit does not follow the continuous separatrix trajectory exactly, we find there is a finite range of parameters with trajectories close to the continuous heteroclinic orbit, and approaching the upper homogeneous state before returning to the lower one again. This *heteroclinic tangle* was shown in [18,19] to lead to a *snaking bifurcation diagram* where there is an infinite number of folds in the continuation of discrete solitons as one approaches the

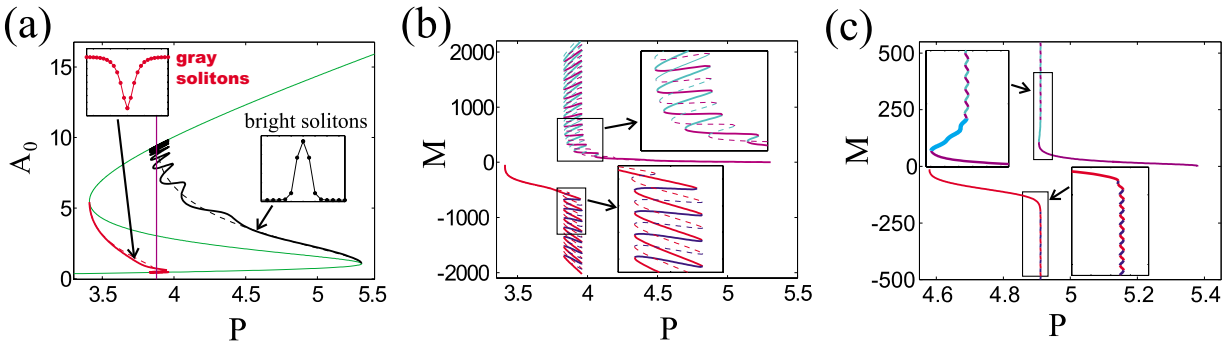

FIG. 2. (Color online) (a) The bifurcation diagram for on-site discrete solitons are shown in (a) for gray and bright solitons by the red and black lines, correspondingly, with the green line representing homogeneous states and the thin magenta line showing the Maxwell point. (b) The same information depicted as M vs P plane by solid lines. Dashed lines show the bifurcation diagrams for off-site solitons. Red and magenta colors show the unstable regions of gray and bright solitons, correspondingly. Blue and cyan lines show the stable regions. The parameters are $\delta=-0.3$, $\alpha=10$, $c=0.5$. (c) The bifurcation diagram $M(P)$ for the lossy case $\delta=-0.3+0.8i$ with the coupling strength $c=1.5$. The thicker line in the upper insertion shows the part of the bifurcation curve which is stable even in the continuum limit.

limit of the discrete heteroclinic connection (pair of fronts). This creates a finite width of P values known as a *pinning region* [20] where there is an infinite number of discrete solitons for the same pump. This is illustrated in Figs. 1(a) and 1(b), where the dark and gray (red) circles represent two different on-site discrete bright solitons at the same pump. The pinning region is found to become wider as the coupling strength is decreased. The same arguments apply to the case of gray solitons. In Fig. 2(a) bifurcation diagrams are depicted for moderate coupling $c=0.5$. The snaking of both the bright and gray soliton branches around the Maxwell point is clear. The observation of snaking bifurcation diagrams in the system under consideration can be anticipated from the work of Refs. [18,19], which consider heteroclinic tangles in Poincaré maps around periodic structures in continuous systems.

To further analyze the snaking it is helpful to show bifurcation diagrams for the norm $M=\Sigma_n(|A_n|^2-|A_\infty|^2)$, which is a discrete analog of the total soliton power taken relative to the background, see Fig. 2(b). Solid thick red and blue curves show the continuation of the on-site gray solitons. The thinner dashed lines show the continuation of the off-site gray soliton. One can see that the norm M is always negative for gray solitons. Solid thick magenta and cyan lines correspond to the on-site bright soliton and the thinner dashed one to the off-site bright solitons. It is seen that in this case the norm M is positive. Let us note here that in the black and white version of the figure the red and cyan lines look lighter than the magenta and blue lines. Comparing Fig. 2(a) and Fig. 2(b) we notice that when the pump approaches the Maxwell point the field amplitude in the soliton center stops growing, but the absolute value of M continues to grow as the soliton width approaches infinity. Every new fold of the bifurcation curve corresponds to the increase of the soliton width by one site.

Figure 2 also shows the stability of the discrete solitons. The stable soliton branches are shown by the blue and cyan curves, and the unstable ones by the red and magenta colors. The stability has been studied by numerical calculation of the spectrum of the system linearized about the soliton and by direct numerical simulations. The latter have revealed two distinct instability scenarios. In both cases the soliton breaks into two moving fronts, which can either move away from the soliton center and one from another or toward it and toward each other. In the former case the homogeneous states nearest to the soliton center fills the cavity. In the latter case the fronts collide and annihilate and the cavity is filled by the homogeneous state, which served as the soliton background. The above scenarios are valid for both bright and gray solitons. Importantly, we found infinitely many stable solitons, both bright and gray, on-site and off-site, inside the pinning region. The region of infinite multistability of soliton states becomes wider in the anticontinuum limit, $c\to 0$, clearly indicating that the discreteness is the primary reason behind the stabilization mechanism. While, in the continuum limit, these solitons can be considered as unstable bound states of traveling fronts, the discreteness provides a Peierls-Nabarro barrier preventing the front motion and thus stabilizing the solitons in a proximity of the Maxwell point.

Now we briefly discuss the influence of linear losses on the cavity solitons: Im $\delta>0$. The presence of losses means that we can no longer assume A_n to be real, and hence the stationary version of Eq. (1) becomes a four-dimensional map. This map is not conservative, but crucially is still *reversible* in the sense of Ref. [21], and so homoclinic trajectories have the same co-dimension as the Hamiltonian case. We found that small losses do not significantly change the solutions discussed so far; see the bifurcation diagram in Fig. 2(c). The complete details will be presented elsewhere, but perhaps the most important, though not unexpected, observation is that sufficiently large losses can cause the high-intensity homogeneous state to have complex multipliers, i.e., it becomes a saddle focus. This in turn opens the possibility to form stable bound states of localized structures.

We should also mention the possibility of experimental observations of the localized states of light discussed above. Recent technology has enabled the creation of resonators with extremely high Q factor; see, for example, Refs. [22,23]. The advantage of low losses is obvious in optical information processing systems, both in terms of quality of signal and power consumption. We note that previously observed discrete cavity solitons in Kerr media have $\delta>0$ in

our notation, and any gray solitons require finite dissipation to be observable [12,13] and indeed can be shown in the continuum limit to cease to exist when the losses tend to zero. In contrast, the solitons we have found for $\delta<0$ are fundamentally different and rely on the saturable nonlinearity. Another interesting feature of our results is the infinite multiplicity of states that have distinct, quantized values of the energy measure M, for pump values that are tuned to lie close to the Maxwell point. This property is particularly appealing for the possible creation of a multiple-state all-optical information processing system.

This work has been supported by EPSRC Grant No. EP/D079225/1.

[1] U. Peschel, D. Michaelis, and C. O. Weiss, IEEE J. Quantum Electron. **39**, 51 (2003).
[2] D. V. Skryabin, Phys. Rev. E **60**, R3508 (1999).
[3] W. J. Firth, L. Columbo, and A. J. Scroggie, Phys. Rev. Lett. **99**, 104503 (2007).
[4] J. Burke and E. Knobloch, Phys. Lett. A **360**, 681 (2006).
[5] A. Yochelis, J. Burke, and E. Knobloch, Phys. Rev. Lett. **97**, 254501 (2006).
[6] G. Kozyreff and S. J. Chapman, Phys. Rev. Lett. **97**, 044502 (2006).
[7] T. Kapitula, P. G. Kevrekidis, and R. Carretero-Gonzalez, Physica D **233**, 112 (2007).
[8] H. Susanto, P. G. Kevrekidis, B. A. Malomed, R. Carretero-Gonzalez, and D. J. Frantzeskakis, Phys. Rev. E **75**, 056605 (2007).
[9] Z. Shi and J. Yang, Phys. Rev. E **75**, 056602 (2007).
[10] J. Wang, J. Yang, and Zh. Chen, Phys. Rev. A **76**, 013828 (2007).
[11] D. Pelinovsky and P. G. Kevrekidis, Physica D **212**, 1 (2005).
[12] U. Peschel, O. Egorov, and F. Lederer, Opt. Lett. **29**, 1909 (2004); O. A. Egorov and F. Lederer, Phys. Rev. A **76**, 053816 (2007).
[13] O. A. Egorov, F. Lederer, and Yu. S. Kivshar, Opt. Express **15**, 4149 (2007).
[14] A. Yulin, D. V. Skryabin, and P. St. J. Russell, Opt. Express **13**, 3529 (2005); A. Vladimirov *et al.*, *ibid.* **13**, 1 (2006).
[15] D. Gomila and G. L. Oppo, Phys. Rev. A **76**, 043823 (2007).
[16] B. Fiedler and J. Scheurle, Mem. Am. Math. Soc. **119**, R8 (1996).
[17] J. Guckenheimer and P. Holmes, *Nonlinear Oscillations, Dynamical Systems and Bifurcations of Vector Fields* (Springer-Verlag, Berlin, 1983).
[18] P. D. Wood and A. R. Champneys, Physica D **129**, 147 (1999).
[19] G. W. Hunt, M. A. Peletier, A. R. Champneys, P. D. Wood, M. Ahmer Wadee, C. J. Budd, and G. J. Lord, Nonlinear Dyn. **21**, 3 (2000).
[20] Y. Pomeau, Physica D **23**, 3 (1986).
[21] J. S. W. Lamb and J. A. G. Roberts, Physica D **112**, 1 (1998).
[22] D. K. Armani, T. J. Kippenberg, S. M. Spillane, and K. J. Vahala, Nature (London) **421**, 925 (2003).
[23] B. S. Song, S. Noda, T. Asano, and Y. Akahane, Nat. Mater. **4**, 207 (2005).